

Nonmesonic weak decay of Λ hypernuclei within a nuclear matter framework.

E. Bauer

Departamento de Física, Universidad Nacional de La Plata,

C. C. 67, 1900 La Plata, Argentina and

Instituto de Física La Plata, CONICET, 1900 La Plata, Argentina

Abstract

The nonmesonic weak decay of Λ hypernuclei is studied using nuclear matter. We have developed a formalism which gives a microscopic interpretation of the process of emission of particles originated in this decay. More specifically, our scheme provides a unified treatment of $\Gamma(\Lambda N \rightarrow NN)$ and N_N (N_{NN}), the Λ non-mesonic weak decay widths and the number of emitted particles (pair of particles) of kind N (NN), respectively. We have also evaluated for the first time the quantum interference terms between the n - and p -induced weak decay amplitudes. Explicit expressions for N_N and N_{NN} are shown within the ring approximation. Using the local density approximation together with the ring approximation, we report results for the decay of the ${}_{\Lambda}^{12}\text{C}$ hypernucleus. We have obtained values for the ratio N_n/N_p (N_{nn}/N_{np}) in the range 1.4 – 1.6 (0.2 – 0.3), where no energy threshold have been employed. The n - and p -induced interference terms modify in less than $\sim 3\%$ these results.

PACS number: 21.80.+a, 25.80.Pw.

Keywords: Λ -hypernuclei, Non-mesonic decay of hypernuclei, Γ_n/Γ_p ratio.

I. INTRODUCTION

The physics of hypernuclei has started in 1952 by the observation of the first hypernucleus through its decays [1]. Since then, the subject has grown and in the present contribution we are concern with a particular topic of the hypernuclei physics: the weak decay of Λ -hypernuclei. For review articles one can see [2, 3]. Many theoretical and experimental [4, 5, 6, 7, 8, 9, 10, 11, 12], efforts have been developed to understand the physics beyond this decay. The two main decay mechanisms are: the Mesonic decay (M), where the decay reaction is $\Lambda \rightarrow \pi N$, that is, the Λ inside the hypernucleus decays into a pion and a nucleon. The second is named Non-Mesonic decay (NM). There are several reactions which contribute to the NM -decay and the simplest one is $\Lambda N \rightarrow NN$. Any of both reactions can occur when a hypernucleus decays. However, the kinematical conditions of the emitted nucleons are very different between the mesonic and the non-mesonic decays. While in the mesonic decay, the momentum carried by the nucleon is of the order of 100 MeV/c, in the NM case, this value is 400 MeV/c (assuming that the two emitted nucleons have the same momentum). This has a strong effect on the values of the corresponding decay widths: the mesonic one (Γ_M), is inhibited by the Pauli blocking. In this work, we focus on the non-mesonic decay width (Γ_{NM}) of Λ -hypernuclei.

For the NM -decay the transition rates can be stimulated either by protons, $\Gamma_p \equiv \Gamma(\Lambda p \rightarrow np)$, or by neutrons, $\Gamma_n \equiv \Gamma(\Lambda n \rightarrow nn)$. The total NM -decay rate is then $\Gamma_{NM} = \Gamma_n + \Gamma_p$. The theory fairly accounts for the experimental values of the total transition rate. There are two quantities which remain not fully understood yet. The first one is the ratio $\Gamma_{n/p} \equiv \Gamma_n/\Gamma_p$, which is discussed soon. The other one is the asymmetry of the protons emitted in the NM -decay of polarized hypernuclei. In this case, the data indicates a value closer to zero, while the theory predicts a large negative number. In the present work, however, we will not deal with the asymmetry.

The ratio $\Gamma_{n/p}$ is evaluated using many theoretical models. The first microscopic scheme has been proposed by Adams [13], who has used the nuclear matter framework, one pion exchange model (OPE), the $\Delta T = 1/2$ piece of the $\Lambda N\pi$ coupling and short range correlations (SRC). The OPE produces ratios in the interval 0.05-0.20, well below data. At variance, Γ_{NM} is well reproduced by OPE. From this point, a huge theoretical effort has been devoted to find a formalism which increases Γ_n and decreases Γ_p . Let us group them as the ones

which care about: *i*) the transition potential: the OPE can be improved by considering heavier mesons than the pion. This $\Lambda N \rightarrow NN$ -transition potential is known as one meson exchange model (OME) and it has been employed in several works [14, 15, 16, 17, 18, 19]. *ii*) The inclusion of interaction terms that violates the isospin $\Delta T = 1/2$ rule has been considered in [3, 20, 21, 22, 23, 24]. *iii*) the addition of two-body induced decay mechanism stemming from ground state correlation of the hypernuclei [25, 26, 27, 28, 29, 30]. In point *ii*), it should be observed that the quark degree of freedom allows for both $\Delta T = 1/2$ and $\Delta T = 3/2$ transitions. All theoretical models consistently obtain values for $\Gamma_{n/p}$ smaller than 0.5 for medium and heavy hypernuclei. In the experimental side, all measurements suggest values greater than 0.5. This discrepancy is usually called the $\Gamma_{n/p}$ -puzzle. Recently, it has been suggested that the origin of this inconsistency comes from the ambiguities in the interpretation of data, rather than in our poor understanding of the weak decay mechanisms [27, 31, 32, 33]. In these works, the intranuclear cascade code (INC) has been developed, which is a semi-phenomenological approach where first the Λ -weak decay is evaluated microscopically and afterwards the nucleons produced in the decay are followed in a semi-classical manner until they leave the nucleus. By means of this emulation of the physical conditions of the hypernuclear decay, a more accurate agreement between the theoretical results and the data is achieved.

Beyond all these theoretical and experimental labor, the effect of the nuclear structure on the calculation of Γ_{NM} is less or even poorly discussed. Oset and Salcedo [34] have developed the polarization propagator method (PPM), which allows a unified treatment of the mesonic and the nonmesonic-decay channels. Nuclear correlations are included through the ring approximation, which is the direct part of the RPA. The PPM has been further developed in Refs. [17, 26, 27, 28]. In a similar spirit of the PPM, Alberico et al. [29] have employed the bosonic loop expansion (BLE) formalism, which is particularly suitable when more than two nucleons emerge from the disintegration process. In practice and until now, the strong potential has entered into the evaluation of Γ_n and Γ_p , only by means of the ring approximation and restricted to a $(\pi + \rho)$ -potential with the addition of the Landau-Migdal g' -parameter.

In the present contribution, we address the problem of the theoretical interpretation of data. This is done within a fully microscopic model, which, as a first step, is restricted to the ring approximation. We pay special attention to the roll of the quantum interference

terms between the n - and p -induced weak decay amplitudes, which are evaluated in this work for the first time. The paper is organized as follows. In Section II, we discuss the way in which Γ_n/Γ_p is extracted from the experimental measurements. In Section III, we propose a model for the physical observables N_N and N_{NN} . In Section IV, explicit expressions for these observables are given within the ring approximation. Finally, in Sections V and VI, some results and conclusions are given.

II. THE EXTRACTION OF THE RATIO Γ_n/Γ_p FROM DATA

Some recent works suggest a solution of the Γ_n/Γ_p -puzzle (see [31, 32, 33]). However, in this section we do not want to go through this explanation, but to call the attention on some aspects about the extraction of Γ_n/Γ_p from data. Therefore, let us start by presenting a simplified version of the way in which the so-called experimental value of Γ_n/Γ_p is obtained. This brief outline does not pretend to be complete. For a more rigorous analysis, we refer the reader to the experimental works [4, 5, 6, 7, 8, 9, 10, 11, 12] and also to the above mentioned studies. There are two equivalent definitions for the experimental value of Γ_n/Γ_p [31, 32],

$$\frac{\Gamma_n}{\Gamma_p} \equiv \frac{1}{2} \left(\frac{N_n^{\text{wd}}}{N_p^{\text{wd}}} - 1 \right) \quad (2.1)$$

$$\frac{\Gamma_n}{\Gamma_p} \equiv \frac{N_{nn}^{\text{wd}}}{N_{np}^{\text{wd}}} \quad (2.2)$$

where N_N^{wd} is the number of nucleons of kind N produced in the weak decay of the Λ . Analogously, N_{NN}^{wd} is the number of NN pairs. Unfortunately, these primary particles can not be measured. Once these particles are produced, in their way out of the nucleus and due to collisions with other nucleons, they can change energy, direction and charge. These interactions with other nucleons are called Final State Interactions (FSI). Perhaps, one of the simplest nuclear models to deal with the FSI is the ring approximation, where the nuclear residual interaction is replaced by a modified interaction built up from an infinite sum of one particle-one hole bubbles. The first order contributions to the ring series for the Λ -decay are shown in Fig. 1, where we have also drawn a diagram for Γ_N . As an example of the action of the FSI we discuss now the last diagram in Fig. 1, which is of second order in the nuclear residual interaction. To develop this example, let us additionally consider that the primary decay is $\Lambda n \rightarrow nn$. The intermediate bubble can be either a nn^{-1} or a pp^{-1} -pair. We also suppose that this bubble is constituted by a pp^{-1} -pair and that it is on the mass shell. The interpretation of this contribution looks somehow confusing: the primary decay is $\Lambda n \rightarrow nn$, while the final state is np . This np -pair is originated from the action of the strong interaction, after the Λ -weak decay takes place. Then, and as it is already known, the emitted particles depend on the FSI. The ring approximation is only one kind among a huge set of FSI. To express in general terms the effect of FSI, in [31] it is written down a set of equations which represents the number of nucleons of the kind N (where $N=n$ or p),

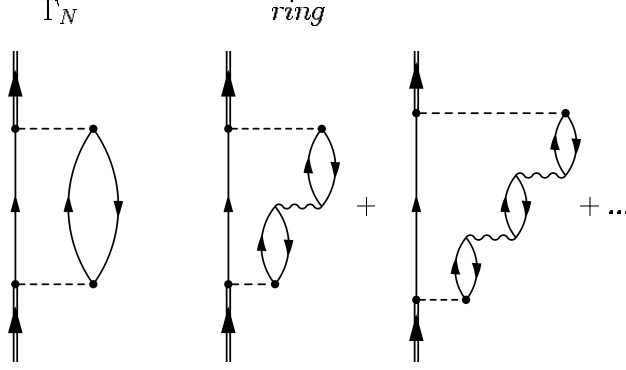


FIG. 1: Goldstone diagrams for Γ_N and the ring series. An up (down) going arrow represents a particle (hole), while an arrow with a double line represents the Λ . The dashed lines represent the full $V^{\Lambda N}$ -transition potential and the intermediate wavy lines represent the strong nuclear potential, V^{NN} .

outgoing the nucleus,

$$N_n = N_n^{1Bn} \bar{\Gamma}_n + N_n^{1Bp} \bar{\Gamma}_p \quad (2.3)$$

$$N_p = N_p^{1Bn} \bar{\Gamma}_n + N_p^{1Bp} \bar{\Gamma}_p, \quad (2.4)$$

where $\bar{\Gamma}_N \equiv \Gamma_N / (\Gamma_n + \Gamma_p)$. Here N_n (N_p) is the number of neutrons (protons) emerging from the nucleus due to the Λ -weak decay, while N_n^{1Bi} (N_p^{1Bi}) is the number of neutrons (protons) coming out of the nucleus which are originated from the $\Lambda i \rightarrow ni$ weak decay ($i = n, p$). In a similar way, for the NN -pairs,

$$N_{nn} = N_{nn}^{1Bn} \bar{\Gamma}_n + N_{nn}^{1Bp} \bar{\Gamma}_p \quad (2.5)$$

$$N_{np} = N_{np}^{1Bn} \bar{\Gamma}_n + N_{np}^{1Bp} \bar{\Gamma}_p \quad (2.6)$$

$$N_{pp} = N_{pp}^{1Bn} \bar{\Gamma}_n + N_{pp}^{1Bp} \bar{\Gamma}_p. \quad (2.7)$$

where the interpretation of the new factors is self-evident. In the last equation, the action of the FSI allows the emission of a pp -pair. For simplicity, in this set of equations we have limited ourselves to nucleons originated from the one-body (1B), decay mechanism (*i.e.* $\Lambda N \rightarrow NN$). The two-body decay mechanism ($\Lambda NN \rightarrow NNN$) is important in the analysis of data, but it is not required for the present discussion.

The Eqs. (2.3-2.4) and Eqs. (2.5-2.7), are one of several proposals to interpret the experimental results. Within this scheme, the dependence on the weak vertex is embodied in

Γ_n and Γ_p . Thus, the $N_N^{1Bn(p)}$ and $N_{NN}^{1Bn(p)}$ -factors depend only on the strong interaction part of the problem and the nuclear model employed to describe the nucleus. Therefore, one working hypothesis of the INC calculation is that the number of emitted particles can be drawn as a sum of product functions: in these products, one factor (Γ_N) contains the entire dependence on the weak vertex. When the strong interaction is turned off, these factors reduce themselves to the number of particles (pairs of particles) of kind N (NN) in the primary decay. In Table I, we quote these values.

TABLE I: Multiplicative factors. The index wd , indicates that the FSI are neglected. As in the one-body weak decay of the Λ there is no pp -pair, we have $(N_{pp}^{1Bn})^{wd}=(N_{pp}^{1Bp})^{wd}=0$.

| | | | |
|-----------------------|-----------------------|-----------------------|-----------------------|
| $(N_n^{1Bn})^{wd}$ | $(N_n^{1Bp})^{wd}$ | $(N_p^{1Bn})^{wd}$ | $(N_p^{1Bp})^{wd}$ |
| 2 | 1 | 0 | 1 |
| $(N_{nn}^{1Bn})^{wd}$ | $(N_{nn}^{1Bp})^{wd}$ | $(N_{np}^{1Bn})^{wd}$ | $(N_{np}^{1Bp})^{wd}$ |
| 1 | 0 | 0 | 1 |

If we replace now the numbers in Table I, into Eqs. (2.3-2.6), we have,

$$N_n^{\text{wd}} = 2\bar{\Gamma}_n + \bar{\Gamma}_p \quad (2.8)$$

$$N_p^{\text{wd}} = \bar{\Gamma}_p, \quad (2.9)$$

and

$$N_{nn}^{\text{wd}} = \bar{\Gamma}_n \quad (2.10)$$

$$N_{np}^{\text{wd}} = \bar{\Gamma}_p \quad (2.11)$$

which lead to the Eqs. (2.1) and (2.2). When FSI are present, we obtain from Eqs. (2.3-2.6),

$$\frac{\Gamma_n}{\Gamma_p} = \frac{N_n^{1Bp} - N_p^{1Bp} \frac{N_n}{N_p}}{N_p^{1Bn} \frac{N_n}{N_p} - N_n^{1Bn}}, \quad (2.12)$$

and

$$\frac{\Gamma_n}{\Gamma_p} = \frac{N_{nn}^{1Bp} - N_{np}^{1Bp} \frac{N_{nn}}{N_{np}}}{N_{np}^{1Bn} \frac{N_{nn}}{N_{np}} - N_{nn}^{1Bn}}. \quad (2.13)$$

Basically, within the INC calculation the so-called experimental value for Γ_n/Γ_p comes from one of these expressions. The Eq. (2.12) is more frequently used than the Eq. (2.13). However, in [3] (see also [32]), it is claimed that the last expression is more convenient, because it reduces the quantum mechanical interferences between n and p -stimulated weak decays. From the experimental point of view, the quantities which can be measured are N_n , N_p , N_{nn} , N_{np} and N_{pp} . Therefore, within the INC calculation the ratio Γ_n/Γ_p is obtained indirectly.

In recent years, there have been many improvements in the experimental side: new and more accurate measurements, independent counts of neutron and protons are performed, etc. The theoretical works have extensively analyzed the weak decay, as stated in the Introduction. Within the INC calculation point of view, the link between the quoted theory and the data, are the $N_N^{1\text{Bn}(p)}$ (or $N_{NN}^{1\text{Bn}(p)}$)-factors. The INC calculation is one of several proposals in the analysis of the experimental points. These other models are found in the experimental works themselves. The simplest approach is the direct use of Eq. (2.1) or (2.2), a model which certainly oversimplified the issue. Among the different models, the INC calculation is perhaps the more elaborated one and its result suggests a solution for the Γ_n/Γ_p -puzzle. For ${}_{\Lambda}^{12}\text{C}$ there is some discrepancy left, but the use of the INC calculation makes the difference smaller than with the employment of other schemes. Moreover, within the INC calculation this difference lays within the uncertainty of the experiment.

Despite assuming that the results from the INC calculation are appropriate enough, nevertheless, a fair question from the theoretical point of view would be, what the microscopic interpretation of the N_N and/or N_{NN} -factors is. In addition, the results from the INC calculation are reliable as far as the quantum interference terms between the n - and p -induced weak decay widths are small. From now on, we will propose an answer for these points, which are the main subjects of the present contribution. A microscopic model for N_N and N_{NN} is given in the next Section. Additionally, in the same Section we attempt to interpret the factors $N_N^{1\text{Bn}(p)}$ and $N_{NN}^{1\text{Bn}(p)}$, from the INC calculation. In Section IV, explicit expressions for all these factors are given using the ring approximation.

III. GENERAL EXPRESSIONS FOR THE N_N AND N_{NN} FACTORS

The starting point to build up microscopic expressions for N_N and N_{NN} are the Eqs. (2.8-2.11). These are the values for N_N and N_{NN} when no FSI are present. Therefore we add to these equations the action of the FSI. To this end, we introduce the quantity $\Gamma_{i,i' \rightarrow j}$. In this function, the indices i, i' refer to the two primary weak decay interactions of each diagram and can have the values $i, i' = n, p$; where by i, i' we mean $\Lambda i, i' \rightarrow n i, i'$. The remaining index, j , is the final state (*i.e.* the emitted nucleons), taking the values: $j = n, nn, np, nnn, nnp, \dots$. For instance, in the example mentioned in the last section, we have $i = i' = n$ and $j = np$. The first obvious constraint over j is the finite number of nucleons in any hypernuclei. Also the charge is conserved and as a result there is always at least one neutron in the final state.

The values for $\Gamma_{i,i' \rightarrow j}$ result from evaluating any possible Goldstone diagram for the Λ -weak decay, where the strong interaction is present. We should be aware that $\Gamma_{i,i' \rightarrow j}$ does not represent only a decay width, but also some interference terms. To understand the origin of these interference terms, the following example can be instructive: we start with the quantity Γ_n , which represents the decay width for the transition amplitude $A_1 : \Lambda n \rightarrow nn$ (for convenience, we have numerated the transition amplitude). In fact, we evaluate the square of this transition amplitude to obtain the final value Γ_n . Once the FSI are incorporated, new transition amplitudes should be included: let us consider the transition amplitude $A_2 : \Lambda p \rightarrow np \rightarrow nn$ [39], where the strong interaction is responsible for the second reaction. This transition amplitude is added to the first one and then the whole expression is squared. From this simple model, four terms come out: the squares of A_1 and A_2 and the two interference terms between A_1 and A_2 . The interference terms are non-zero because the initial and the final states are the same. The first two, can be interpreted as decay widths, but not the interference terms which can be either positive or negative. Besides this simple example, by means of $\Gamma_{i,i' \rightarrow j}$ we represent all terms but the squares of $\Lambda n \rightarrow nn$ and $\Lambda p \rightarrow np$. A second important observation about the interference terms in $\Gamma_{i,i' \rightarrow j}$, is that a particular case of these terms are the ones between the n - and p -induced weak decays. The interference terms between A_1 and A_2 are an example of such contribution. One of the simplest diagrams

[39] A more complete expression would be, $A_2 : \Lambda p(n_b) \rightarrow np(n_b) \rightarrow nn(p_b)$ where the subindex b , indicates bound particles acting as spectators. In this way, the charge conservation is more clearly seen.

for these interference terms, is the first ring diagram in Fig. 1, taking one bubble as a pp^{-1} -pair and the other one as a nn^{-1} -pair. Note also that in this diagram the nuclear strong interaction appears in first order and the sign of the contribution depends on the sign of this interaction. The interference terms in $\Gamma_{i,i' \rightarrow j}$ are pure quantum mechanical effects and the ones with $i \neq i'$, are not contained in the semi-phenomenological INC calculation.

Now, we write down expressions for N_N ,

$$N_n = 2\bar{\Gamma}_n + \bar{\Gamma}_p + \sum_{i, i'=n, p; j} N_{j(n)} \bar{\Gamma}_{i, i' \rightarrow j}, \quad (3.1)$$

$$N_p = \bar{\Gamma}_p + \sum_{i, i'=n, p; j} N_{j(p)} \bar{\Gamma}_{i, i' \rightarrow j}, \quad (3.2)$$

and for N_{NN} ,

$$N_{nn} = \bar{\Gamma}_n + \sum_{i, i'=n, p; j} N_{j(nn)} \bar{\Gamma}_{i, i' \rightarrow j}, \quad (3.3)$$

$$N_{np} = \bar{\Gamma}_p + \sum_{i, i'=n, p; j} N_{j(np)} \bar{\Gamma}_{i, i' \rightarrow j}, \quad (3.4)$$

$$N_{pp} = \sum_{i, i'=n, p; j} N_{j(pp)} \bar{\Gamma}_{i, i' \rightarrow j}, \quad (3.5)$$

where the normalization is the same as in Eq. (2.3) (*i. e.* $\bar{\Gamma}_{i, i' \rightarrow j} \equiv \Gamma_{i, i' \rightarrow j} / (\Gamma_n + \Gamma_p)$). The factors $N_{j(N)}$ are the numbers of nucleons of the type N in the state j . In the same way, $N_{j(NN)}$ are the numbers of pairs of nucleons of the type NN in the state j . For instance, if $j = nn$, $N_{nn(n)} = 2$, and $N_{nn(p)} = 0$.

Expressions for $N_N^{1B i}$ and $N_{NN}^{1B i}$ are obtained by comparison between Eqs. (2.3-2.7) and Eqs. (3.1-3.5). To this end, the $\Gamma_{i, i' \rightarrow j}$ -terms with $i \neq i'$ must be neglected. We have then,

$$N_N^{1B i} = (N_N^{1B i})^{wd} + \sum_j N_{j(N)} \frac{\Gamma_{i, i \rightarrow j}}{\Gamma_i} \quad (3.6)$$

$$N_{NN}^{1B i} = (N_{NN}^{1B i})^{wd} + \sum_j N_{j(NN)} \frac{\Gamma_{i, i \rightarrow j}}{\Gamma_i}, \quad (3.7)$$

where in order to reduce the expressions we have used the factors in Table I. As mentioned above, within the INC calculation these factors are independent of the weak vertex. Our expressions fulfilled this requirement only when the transition potential is reduced to one term: in this case, the weak vertex constant is simplified in the ratio $\Gamma_{i, i \rightarrow j} / \Gamma_i$. When the full transition potential is present, then $\Gamma_{i, i \rightarrow j} / \Gamma_i$ has some dependence on the weak vertex. This point is further analyzed in Section V.

Before we end this section, we would like to make a brief comment on the calculations performed in finite hypernuclei. In this case, the weak decay matrix element, required for $\Gamma_{n,(p)}$, is evaluated using finite nucleus wave-functions (WF). These WF can be the harmonic oscillator WF, but also some more elaborate WF: the ones from a BCS-, Tamm-Dancoff-, RPA-calculations or any other model. In any case, these WF represent bound states. After the weak decay takes place, the unbound emitted particles are modelled by nuclear-matter distorted plane-waves. Nuclear correlations between the emitted particles are the FSI, which do not affect the $\Gamma_{n,(p)}$ -result. The FSI should not be confused with nuclear correlations employed in the evaluation of the finite nucleus WF. For instance, the finite nucleus WF can be the RPA-ones and afterwards, the FSI can be implemented using the RPA. In this case, there is no double-counting: first, the RPA is performed within bound particles and then, the nuclear correlations are taken into account between the particles in the continuum.

IV. THE RING APPROXIMATION

In this section we present expressions for the quantities $\Gamma_{i,i' \rightarrow j}$, within the ring approximation. This is done in non-relativistic nuclear matter. Before we show these expressions, it is convenient to outline the derivation of Γ_n and Γ_p . Even though these contributions have been already discussed in [35], we repeat now the main points of that derivation, because this simplifies our presentation. To be consistent with the ring approximation, we neglect the Pauli exchange term also in $\Gamma_{n(p)}$. In $\Gamma_{n(p)}$ only the transition potential $V^{\Lambda N}$ is present, while in the ring approximation, also the strong interaction V^{NN} , is required. Both $V^{\Lambda N}$ and V^{NN} are parameterized as follows,

$$V^{\Lambda N(NN)}(q) = \sum_{\tau_{\Lambda(N)}=0,1} \mathcal{O}_{\tau_{\Lambda(N)}} \mathcal{V}_{\tau_{\Lambda(N)}}^{\Lambda N(NN)}(q), \quad (4.1)$$

where q is the energy-momentum carried by the potential. The isospin dependence is given by,

$$\mathcal{O}_{\tau_{\Lambda(N)}} = \begin{cases} 1, & \text{for } \tau_{\Lambda(N)} = 0 \\ \boldsymbol{\tau}_1 \cdot \boldsymbol{\tau}_2, & \text{for } \tau_{\Lambda(N)} = 1 \end{cases} \quad (4.2)$$

The values $\tau = 0, 1$ stand for the isoscalar and isovector parts of the interaction, respectively. The spin and momentum dependence of the transition potential is,

$$\begin{aligned} \mathcal{V}_{\tau_{\Lambda}}^{\Lambda N}(q) = & (G_F m_{\pi}^2) \{ S_{\tau_{\Lambda}}(q) \boldsymbol{\sigma}_1 \cdot \hat{\mathbf{q}} + S'_{\tau_{\Lambda}}(q) \boldsymbol{\sigma}_2 \cdot \hat{\mathbf{q}} + P_{L,\tau_{\Lambda}}(q) \boldsymbol{\sigma}_1 \cdot \hat{\mathbf{q}} \boldsymbol{\sigma}_2 \cdot \hat{\mathbf{q}} + P_{C,\tau_{\Lambda}}(q) + \\ & + P_{T,\tau_{\Lambda}}(q) (\boldsymbol{\sigma}_1 \times \hat{\mathbf{q}}) \cdot (\boldsymbol{\sigma}_2 \times \hat{\mathbf{q}}) + i S_{V,\tau_{\Lambda}}(q) (\boldsymbol{\sigma}_1 \times \boldsymbol{\sigma}_2) \cdot \hat{\mathbf{q}} \}, \end{aligned} \quad (4.3)$$

where the quantities $S_{\tau_{\Lambda}}(q)$, $S'_{\tau_{\Lambda}}(q)$, $P_{L,\tau_{\Lambda}}(q)$, $P_{C,\tau_{\Lambda}}(q)$, $P_{T,\tau_{\Lambda}}(q)$ and $S_{V,\tau_{\Lambda}}(q)$ contain short range correlations (SRC) and are given in Appendix B of [35]. They are built up from the full one-meson-exchange model, which involves the complete pseudoscalar and vector meson octets ($\pi, \eta, K, \rho, \omega, K^*$). The S (P)-terms are the parity violating (parity conserving) terms of the transition potential.

The spin and momentum dependence of the nuclear residual interaction is drawn as,

$$\mathcal{V}_{\tau_N}^{NN}(q) = \left(\frac{f_{\pi}^2}{m_{\pi}^2} \right) \{ \mathcal{V}_{C,\tau_N}(q) + \mathcal{V}_{L,\tau_N}(q) \boldsymbol{\sigma}_1 \cdot \hat{\mathbf{q}} \boldsymbol{\sigma}_2 \cdot \hat{\mathbf{q}} + \mathcal{V}_{T,\tau_N}(q) (\boldsymbol{\sigma}_1 \times \hat{\mathbf{q}}) \cdot (\boldsymbol{\sigma}_2 \times \hat{\mathbf{q}}) \}, \quad (4.4)$$

where the functions $\mathcal{V}_{C,\tau_N}(q)$, $\mathcal{V}_{L,\tau_N}(q)$ and $\mathcal{V}_{T,\tau_N}(q)$ are adjusted to reproduce any effective OME-nuclear residual interaction. In addition, following the same procedure as for $\mathcal{V}_{\tau_{\Lambda}}^{\Lambda N}(q)$ (see [35]), SRC can be incorporated into $\mathcal{V}_{\tau_N}^{NN}(q)$.

We go back to the evaluation of the Γ 's (both $\Gamma_{n(p)}$ and $\Gamma_{i,i'\rightarrow j}$). It is more suitable to work with a partial decay width $\Gamma(k, k_{F_n}, k_{F_p})$, instead of Γ , where, k is the Λ energy-momentum, k_{F_n} and k_{F_p} are the Fermi momentum for neutrons and protons, respectively. To evaluate $\Gamma(k)$ for a particular nucleus one uses either an effective Fermi momentum or the Local Density Approximation (LDA) [34]. In this work the LDA is employed. In this case, k_{F_n} and k_{F_p} become position-dependent and are defined as $k_{F_{n(p)}}(r) = \hbar c(3\pi^2\rho_{n(p)}(r)/2)^{1/3}$, where $\rho_n(r) = \rho(r)N/(N+Z)$ and $\rho_p(r) = \rho(r)Z/(N+Z)$, with $\rho(r)$, N and Z being, respectively, the density profile, number of neutrons and number of protons of the nuclear core of the hypernucleus. In the last case, it is equivalent to write the function $\Gamma(k, k_{F_n}, k_{F_p})$ in terms of the densities as $\Gamma(k, \rho_n(r), \rho_p(r))$. The LDA reads,

$$\Gamma(k) = \int d\mathbf{r} \Gamma(k, \rho_n(r), \rho_p(r)) |\psi_\Lambda(\mathbf{r})|^2 \quad (4.5)$$

where for the Λ wave function $\psi_\Lambda(\mathbf{r})$, we take the $1s_{1/2}$ wave function of a harmonic oscillator. This decay width can be seen as the k -component of the Λ decay width. The total decay width is obtained by averaging over the Λ momentum distribution, $|\tilde{\psi}_\Lambda(\mathbf{k})|^2$, as follows,

$$\Gamma = \int d\mathbf{k} \Gamma(k) |\tilde{\psi}_\Lambda(\mathbf{k})|^2 \quad (4.6)$$

where $\tilde{\psi}_\Lambda(\mathbf{k})$ is the Fourier transform of $\psi_\Lambda(\mathbf{r})$ and $k_0 = E_\Lambda(\mathbf{k}) + V_\Lambda$, being V_Λ the binding energy for the Λ .

A. The evaluation of Γ_n and Γ_p

We give now expressions for the partial decay widths $\Gamma_{n(p)}(k, k_{F_n}, k_{F_p})$. We should evaluate the first diagram in Fig. 2 and 3, named as Γ_i . For convenience, in these figures we also present the ring contributions to $\Gamma_{i,i'\rightarrow j}$. We assign the names $p1$, pi and hi to the particle between the Λ 's and the particle and hole in the bubble, respectively. In order to perform the summation over spin and isospin quantum numbers, it is more adequate to rewrite the transition rates in the form [35],

$$\Gamma_{t_{hi}}(k, k_{F_n}, k_{F_p}) = \sum_{\tau, \tau'=0,1} \mathcal{T}_{t_{hi}; \tau\tau'} \tilde{\Gamma}_{\tau\tau'}(k, k_{F_n}, k_{F_p}) \quad (4.7)$$

where we distinguish between the proton ($t_{hi} = 1/2$) and the neutron induced ($t_{hi} = -1/2$) decay rates. We have introduced the function,

$$\mathcal{T}_{t_{hi}; \tau\tau'} = \sum_{t_{p1}, t_{pi}} \langle t_\Lambda | \mathcal{O}_\tau | t_{p1} t_{pi} t_{hi} \rangle \langle t_{p1} t_{pi} t_{hi} | \mathcal{O}_{\tau'} | t_\Lambda \rangle, \quad (4.8)$$

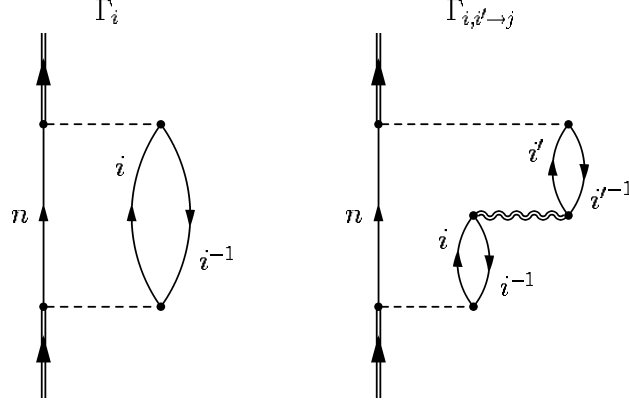


FIG. 2: Goldstone diagrams for Γ_i and $\Gamma_{i,i' \rightarrow j}$, respectively. In both diagrams, the vertex in the Λ -decay is connected to a neutron. In the second diagram, the double-wavy line is the dressed potential \tilde{V}^{NN} , which is described soon, in Eq. (4.13).

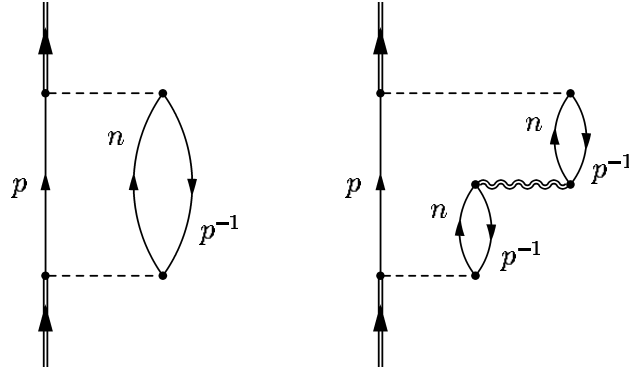


FIG. 3: The same as in Fig. 2, but with a proton in the Λ -decay vertex.

to account for the isospin matrix elements. The partial decay width as a function of the isospin of the transition potential, is,

$$\tilde{\Gamma}_{\tau\tau'}(k, k_{F_n}, k_{F_p}) = (G_F m_\pi^2)^2 \frac{1}{(2\pi)^2} \int d\mathbf{p}_1 \theta(q_0) \theta(|\mathbf{p}_1| - k_{F_p}) \mathcal{S}_{\tau\tau'}(q) (4 \text{Im}(\Pi^0 t_{pi} t_{hi}(q))), \quad (4.9)$$

where,

$$\begin{aligned} \mathcal{S}_{\tau\tau'}(q) = & 4 \{ S_\tau(q) S_{\tau'}(q) + S'_\tau(q) S'_{\tau'}(q) + P_{L,\tau}(q) P_{L,\tau'}(q) + P_{C,\tau}(q) P_{C,\tau'}(q) + \\ & + 2 P_{T,\tau}(q) P_{T,\tau'}(q) + 2 S_{V,\tau}(q) S_{V,\tau'}(q) \} \end{aligned} \quad (4.10)$$

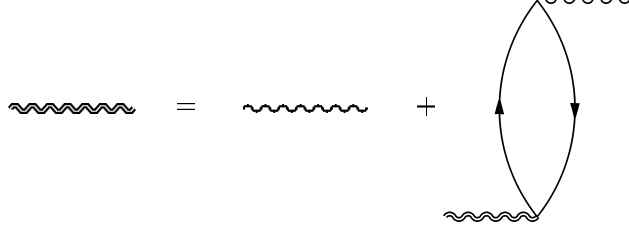


FIG. 4: Diagrammatic representation of the Dyson equation. A wavy line represents the nuclear interaction, V^{NN} , while a double-wavy line is the dressed interaction \tilde{V}^{NN} .

and

$$\Pi^0 t_{pi} t_{hi}(q) = \frac{-1}{(2\pi)^3} \int d\mathbf{p}_i \frac{\theta(|\mathbf{p}_i| - k_{Fpi})\theta(k_{Fhi} - |\mathbf{h}_i|)}{q_0 - (E_N(\mathbf{p}_i) - E_N(\mathbf{h}_i)) + i\eta}, \quad (4.11)$$

is the polarization propagator. Here E_N is the nucleon total free energy. The (k, k_{F_n}, k_{F_p}) -dependence of the partial widths $\tilde{\Gamma}_{\tau\tau'}(k, k_{F_n}, k_{F_p})$ is eliminated by means of the Eqs. (4.6) and (4.5). By performing now the isospin summation, the final result from Eq. (4.7) is,

$$\begin{aligned} \Gamma_n &= \tilde{\Gamma}_{11} + \tilde{\Gamma}_{00} + \tilde{\Gamma}_{01} + \tilde{\Gamma}_{10} \\ \Gamma_p &= 5\tilde{\Gamma}_{11} + \tilde{\Gamma}_{00} - (\tilde{\Gamma}_{01} + \tilde{\Gamma}_{10}), \end{aligned} \quad (4.12)$$

where the presence of terms $\tilde{\Gamma}_{\tau\tau'}$ with $\tau \neq \tau'$ is a consequence of the restriction in the isospin sum. For the non-mesonic decay width, $\Gamma_{NM} = \Gamma_n + \Gamma_p$, these terms cancel out.

B. The evaluation of $\Gamma_{i,i' \rightarrow j}$

In the ring approximation, diagrams with one particle-one hole bubbles are summed up to infinite order. The lowest order contribution to the ring series is of first order in the strong interaction, V^{NN} and it is shown as the first ring diagram in Fig. 1. To obtain all the other contributions, the basic idea is to replace V^{NN} , by a dressed interaction, \tilde{V}^{NN} , obtained as a result of the sum of the ring series. This process is sketched in Fig. 4, which is a representation of the Dyson equation,

$$\tilde{\mathcal{V}}_{C, (L, T); \tau_N} = \mathcal{V}_{C, (L, T); \tau_N} + \tilde{\mathcal{V}}_{C, (L, T); \tau_N} C_{s, t} \Pi_{pi, hi}^0 (f_\pi^2/m_\pi^2) \mathcal{V}_{C, (L, T); \tau_N} \quad (4.13)$$

where the constant $C_{s, t}$ comes from the sum over spin-isospin and it is specified soon. We have shorten the notation for the polarization propagator. The way in which the nuclear

interaction is displayed in Eqs. (4.1) and (4.4), has the advantage that there is no-interference between the central (C), spin-longitudinal (L) and spin-transverse (T) terms, neither nor between the isoscalar ($\tau = 0$) and isovector ($\tau = 1$) ones. The solution for the Dyson equation is,

$$\tilde{\mathcal{V}}_{C,(L,T);\tau_N} = \frac{\mathcal{V}_{C,(L,T);\tau_N}}{1 - (f_\pi^2/m_\pi^2) \mathcal{V}_{C,(L,T);\tau_N} C_{s,t} \Pi_{pi,hi}^0}, \quad (4.14)$$

The interaction \tilde{V}^{NN} , is then,

$$\tilde{V}^{NN}(q) = \sum_{\tau_N=0,1} \mathcal{O}_{\tau_N} \tilde{\mathcal{V}}_{\tau_N}^{NN}(q), \quad (4.15)$$

where \mathcal{O}_{τ_N} is defined in Eq. (4.2) and

$$\tilde{\mathcal{V}}_{\tau_N}^{NN}(q) = \left(\frac{f_\pi^2}{m_\pi^2}\right) \{\tilde{\mathcal{V}}_{C,\tau_N}(q) + \tilde{\mathcal{V}}_{L,\tau_N}(q) \boldsymbol{\sigma}_1 \cdot \hat{\mathbf{q}} \boldsymbol{\sigma}_2 \cdot \hat{\mathbf{q}} + \tilde{\mathcal{V}}_{T,\tau_N}(q) (\boldsymbol{\sigma}_1 \times \hat{\mathbf{q}}) \cdot (\boldsymbol{\sigma}_2 \times \hat{\mathbf{q}})\}. \quad (4.16)$$

The replacement of this interaction into the evaluation of a decay width is not straightforward, because of the restrictions in the isospin summation. The isospin, is a crucial ingredient in the construction of $\Gamma_{i,i' \rightarrow j}$. Within the ring approximation, there are only two possible final states: nn or np . Therefore, we should give expressions for eight quantities: $\Gamma_{n,n \rightarrow nn}$, $\Gamma_{n,p \rightarrow nn}$, $\Gamma_{p,n \rightarrow nn}$, $\Gamma_{p,p \rightarrow nn}$ and the remaining four expressions are obtained by replacing the final state nn by np in the former four ones. In Figs. 5 and 6, we show some of the lower order ring-diagrams which contribute to $\Gamma_{i,i' \rightarrow nn}$ and $\Gamma_{i,i' \rightarrow np}$, respectively.

To obtain general expressions for $\Gamma_{i,i' \rightarrow j}$, it is more convenient to work with Figs. 2 and 3, where we show four diagrams: the particle in the Λ -decay vertex is a neutron in the first figure and a proton in the second case. The particle-hole pairs ii^{-1} and $i'i'^{-1}$ in Fig. 2, can take the values nn^{-1} or pp^{-1} . However, the isospin conservation allows only np^{-1} -pairs in the same position in Fig. 3. The same considerations hold for the particle-hole pairs in \tilde{V}^{NN} . Consequently, by choosing adequately the particle-hole pairs and the cut in the diagrams in Fig. 2, we have that the first one, contributes to Γ_n and Γ_p , while the second one does the same to the eight $\Gamma_{i,i' \rightarrow j}$ -functions. At variance, the diagrams in Fig. 3 only play a role in Γ_p and in $\Gamma_{p,p \rightarrow np}$, for the first and second diagrams, respectively.

Using as a guide the diagrams drawn in the second places in Figs. 2 and 3, we build up expressions for $\Gamma_{i,i' \rightarrow j}$. We follow similar steps as in the derivation of Γ_N . In this case, however, we begin with a general expression, using the standard Goldstone-rules for diagrams,

$$\Gamma_{t_{hi}, t_{hi'} \rightarrow j}(k, k_{F_n}, k_{F_p}) = -2 \text{Im} \int \frac{d^4 p_1}{(2\pi)^4} \int \frac{d^4 h_i}{(2\pi)^4} \int \frac{d^4 h_{i'}}{(2\pi)^4} \frac{1}{4} \sum G_{part}(p_1) G_{part}(p_i)$$

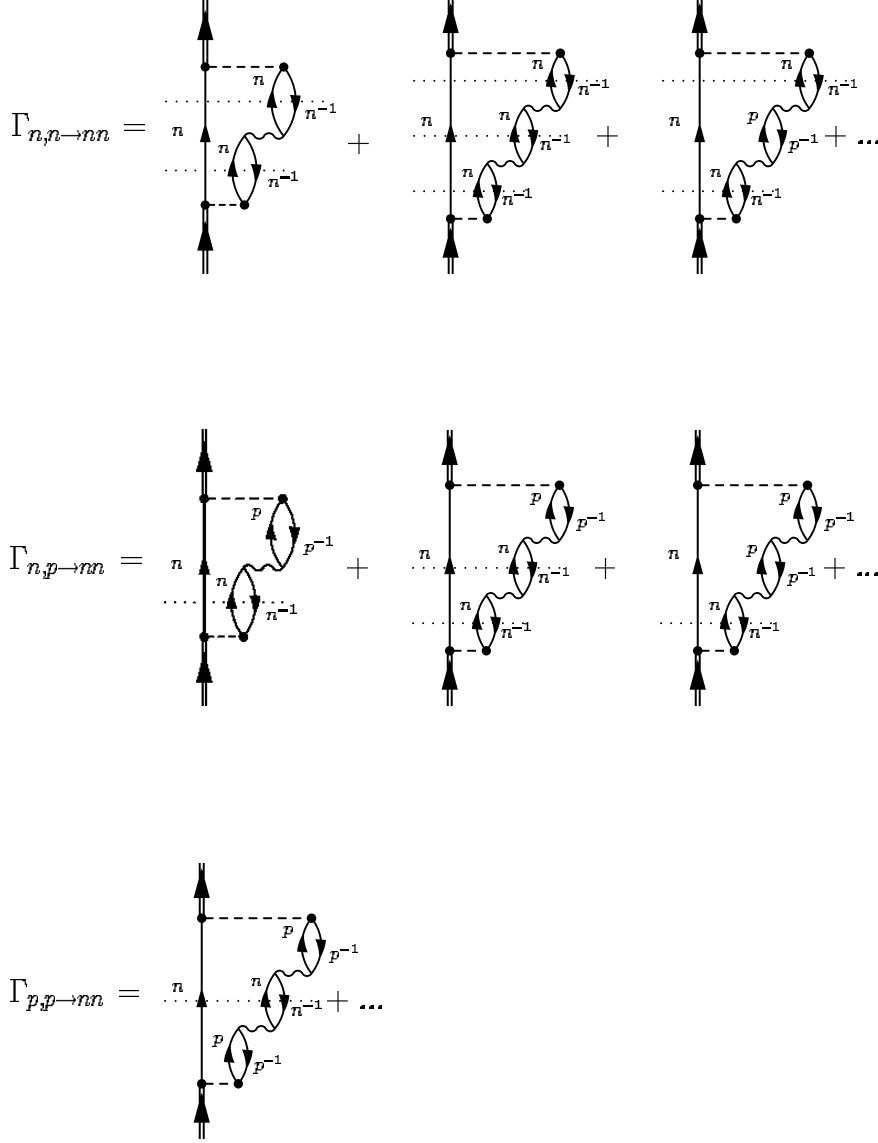


FIG. 5: Goldstone diagrams for $\Gamma_{i,i' \rightarrow nn}$. In this set of diagrams we present some representative examples of this quantity. Here, a dotted line represents the state on the mass shell. A diagram with two or more dotted lines stands for the sum of diagrams with one each. The explicit inclusion of $\Gamma_{p,n \rightarrow nn}$ is omitted, as it is analogous to $\Gamma_{n,p \rightarrow nn}$.

$$\begin{aligned}
& G_{part}(p_{i'}) G_{hole}(h_i) G_{hole}(h_{i'}) \\
& \times \langle \gamma_\Lambda | (V^{\Lambda N}(q))^\dagger | \gamma_{p1} \gamma_{pi'} \gamma_{hi'} \rangle \langle \gamma_{p1} \gamma_{pi'} \gamma_{hi'} | \tilde{V}^{NN}(q) | \gamma_{p1} \gamma_{pi} \gamma_{hi} \rangle \\
& \times \langle \gamma_{p1} \gamma_{pi} \gamma_{hi} | V^{\Lambda N}(q) | \gamma_\Lambda \rangle.
\end{aligned} \tag{4.17}$$

For simplicity, γ_l represents the spin (s), isospin (t) and energy-momentum of the particle

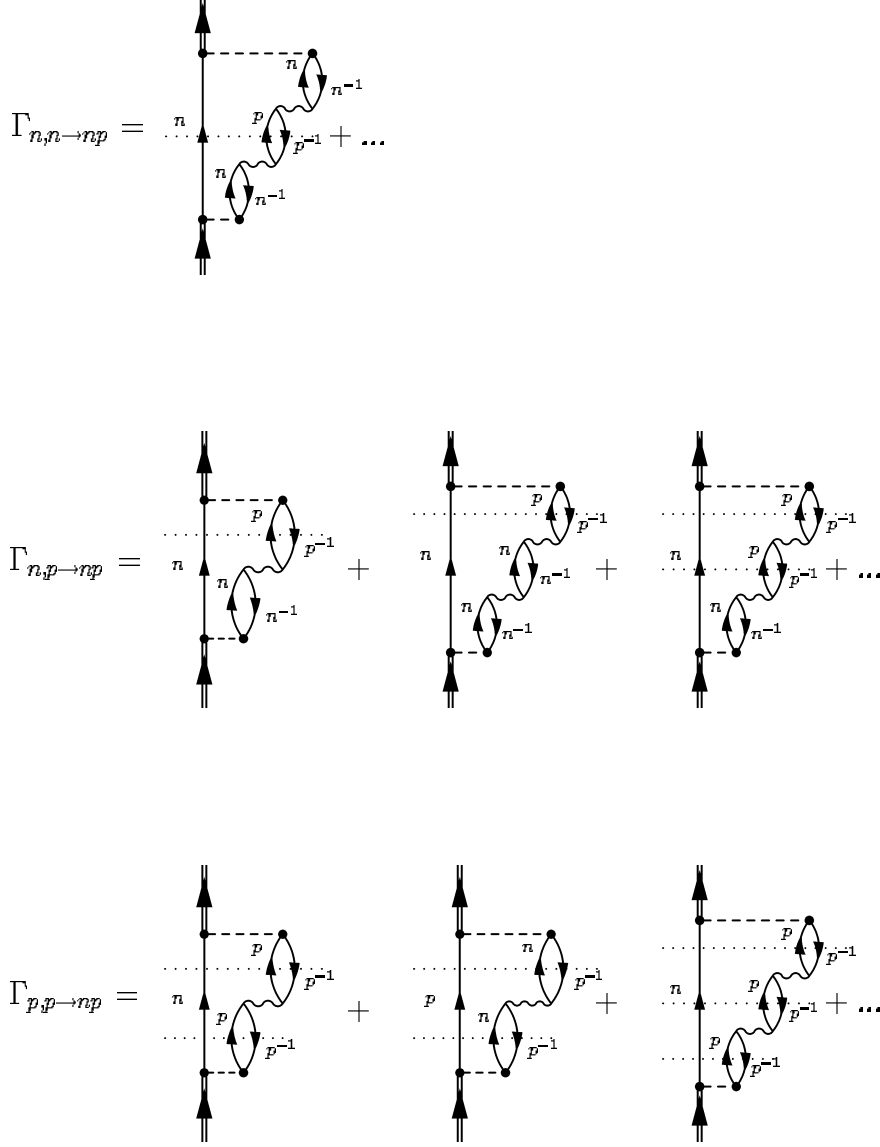


FIG. 6: The same as in Fig. 5, but for $\Gamma_{i,i' \rightarrow np}$.

l. Although the meaning of the subindices pi and hi (pi' and hi'), refers to the particle-hole pair ii^{-1} ($i'i'^{-1}$) in Fig. 2, this expression is also valid for the second diagram in Fig. 3. Using the same notation as in Eq. (4.9), p_1 represents the particle between both Λ' s. From the energy-momentum conservation, we have, $q = k - p_1$, $p_i = q + h_i$ and $p_{i'} = q + h_{i'}$. The summation runs over all spins, while the isospin sum can not be specified until one sets the final state j . The particle and the hole propagators are, respectively,

$$G_{part}(p) = \frac{\theta(|\mathbf{p}| - k_F)}{p_0 - E_N(\mathbf{p}) - V_N + i\varepsilon} \quad (4.18)$$

and

$$G_{hole}(h) = \frac{\theta(k_F - |\mathbf{h}|)}{h_0 - E_N(\mathbf{h}) - V_N - i\varepsilon}, \quad (4.19)$$

where V_N is the nucleon binding energy. We re-write Eq. (4.17) in terms of partial decay widths as follows,

$$\Gamma_{i,i' \rightarrow j}(k, k_{F_n}, k_{F_p}) = \sum_{\tau_\Lambda, \tau_N, \tau'_\Lambda=0,1} \mathcal{T}_{t_{hi}, t_{hi'}; \tau_\Lambda, \tau_N, \tau'_\Lambda} \tilde{\Gamma}_{\tau_\Lambda, \tau_N, \tau'_\Lambda}^{i,i' \rightarrow j}(k, k_{F_n}, k_{F_p}) \quad (4.20)$$

where

$$\mathcal{T}_{t_{hi}, t_{hi'}; \tau_\Lambda, \tau_N, \tau'_\Lambda} = \sum \langle t_\Lambda | \mathcal{O}_{\tau'_\Lambda} | t_{p1} t_{pi'} t_{hi'} \rangle \langle t_{p1} t_{pi'} t_{hi'} | \mathcal{O}_{\tau_N} | t_{p1} t_{pi} t_{hi} \rangle \langle t_{p1} t_{pi} t_{hi} | \mathcal{O}_{\tau_\Lambda} | t_\Lambda \rangle. \quad (4.21)$$

Now the summation runs only over isospin, with the same consideration as in Eq. (4.17). When performing the energy integrations in Eq. (4.17), one keeps only two-particles on the mass shell (more details are given soon). The partial decay widths as function of the isospin of the transition potential, are defined as,

$$\tilde{\Gamma}_{\tau \tau_N \tau'}^{i,i' \rightarrow j, n}(k, k_{F_n}, k_{F_p}) = (G_F m_\pi^2)^2 \left(\frac{f_\pi^2}{m_\pi^2} \right) \frac{1}{(2\pi)^2} \int d\mathbf{p}_1 \theta(q_0) \theta(|\mathbf{p}_1| - k_{F_n}) \tilde{\mathcal{S}}_{\tau \tau_N \tau'}^{i,i' \rightarrow j, n}(q) \quad (4.22)$$

for the second diagram in Fig. 2, where the super-index n refers to the particle in the Λ -vertex (which is explicitly indicated in the step function). For the second diagram in Fig. 3, we have,

$$\tilde{\Gamma}_{\tau \tau_N \tau'}^{i,i' \rightarrow j, p}(k, k_{F_n}, k_{F_p}) = (G_F m_\pi^2)^2 \left(\frac{f_\pi^2}{m_\pi^2} \right) \frac{1}{(2\pi)^2} \int d\mathbf{p}_1 \theta(q_0) \theta(|\mathbf{p}_1| - k_{F_p}) \tilde{\mathcal{S}}_{\tau \tau_N \tau'}^{i,i' \rightarrow j, p}(q), \quad (4.23)$$

where the meaning of the super-index p is self-evident. We define the \mathcal{S} -functions as (for details, see the Appendix),

$$\begin{aligned} \tilde{\mathcal{S}}_{\tau \tau_N \tau'}^{i,i' \rightarrow j, n}(q) = & -\{(S'_\tau S'_{\tau'} + P_{C,\tau} P_{C,\tau'}) \tilde{\mathcal{U}}_{C; \tau_N}^{i,i' \rightarrow j, n}(q) + (S_\tau S_{\tau'} + P_{L,\tau} P_{L,\tau'}) \tilde{\mathcal{U}}_{L; \tau_N}^{i,i' \rightarrow j, n}(q) + \\ & + 2(S_{V,\tau} S_{V,\tau'} + P_{T,\tau} P_{T,\tau'}) \tilde{\mathcal{U}}_{T; \tau_N}^{i,i' \rightarrow j, n}(q)\} \end{aligned} \quad (4.24)$$

and

$$\begin{aligned} \tilde{\mathcal{S}}_{\tau \tau_N \tau'}^{i,i' \rightarrow j, p}(q) = & -\{(S'_\tau S'_{\tau'} + P_{C,\tau} P_{C,\tau'}) \tilde{\mathcal{U}}_{C; \tau_N}^{i,i' \rightarrow j, p}(q) + (S_\tau S_{\tau'} + P_{L,\tau} P_{L,\tau'}) \tilde{\mathcal{U}}_{L; \tau_N}^{i,i' \rightarrow j, p}(q) + \\ & + 2(S_{V,\tau} S_{V,\tau'} + P_{T,\tau} P_{T,\tau'}) \tilde{\mathcal{U}}_{T; \tau_N}^{i,i' \rightarrow j, p}(q)\}, \end{aligned} \quad (4.25)$$

To construct the functions $\tilde{\mathcal{U}}_{C, (L, T); \tau_N}^{i,i' \rightarrow j, n}(q)$ and $\tilde{\mathcal{U}}_{C, (L, T); \tau_N}^{i,i' \rightarrow j, p}(q)$, we first interpret the particle-hole bubbles and the residual interaction, \tilde{V}^{NN} (which contains a sum of particle-hole bubbles), in terms of configurations and the possible final states that they can generate. The

particle-hole bubble is represented by the polarization propagator, $\Pi^0 t_p t_h(q)$, which has a real and an imaginary part. The physical state in any diagram, is determined by the position where the cut of the diagram is done. In practical terms and within the present problem, the imaginary part of the polarization propagator produce the final state, while the real part is related with configurations off the mass shell. By performing the sum over isospin, the polarization propagator is replaced by the sum $(\Pi_{nn}^0 + \Pi_{pp}^0)$ for the $\Gamma_{i,i' \rightarrow j}$ -diagrams in Fig. 2, and by Π_{np}^0 for the ones in Fig. 3. Note that this is done not only for the bubbles explicitly drawn in these figures, but also for the ones inside \tilde{V}^{NN} .

Having in mind these considerations, explicit expressions for the interaction in Eq. (4.14) are obtained as follows. When $j = nn$ the diagrams in Fig. 3 have no contribution, while in Fig. 2, the polarization propagator is replaced by, $(Re\Pi_{nn}^0 + Re\Pi_{pp}^0 + iIm\Pi_{nn}^0)$: we have only retained the imaginary part from the nn^{-1} -bubble. This neutron, together with the one produced in the Λ -decay vertex, give rise to the final nn -state. The pp^{-1} -bubble has a contribution off the mass shell and therefore we keep only the real part of it. In an analogously way, if $j = np$, the polarization propagator is $(Re\Pi_{nn}^0 + Re\Pi_{pp}^0 + iIm\Pi_{pp}^0)$. The diagrams in Fig. 3 contribute only to $j = np$ and in this case the polarization propagator is replaced by, $(Re\Pi_{np}^0 + iIm\Pi_{np}^0)$. From Eq. (4.14) we have, then,

$$\begin{aligned}\tilde{\mathcal{V}}_{nn,C,(L,T);\tau_N} &= \frac{\mathcal{V}_{C,(L,T);\tau_N}}{1 - 2(f_\pi^2/m_\pi^2) \mathcal{V}_{C,(L,T);\tau_N} (Re\Pi_{nn}^0 + Re\Pi_{pp}^0 + iIm\Pi_{nn}^0)}, \\ \tilde{\mathcal{V}}_{np,C,(L,T);\tau_N} &= \frac{\mathcal{V}_{C,(L,T);\tau_N}}{1 - 4(f_\pi^2/m_\pi^2) \mathcal{V}_{C,(L,T);\tau_N} (Re\Pi_{np}^0 + iIm\Pi_{np}^0)} \quad \text{and} \\ \tilde{\mathcal{V}}_{pp,C,(L,T);\tau_N} &= \frac{\mathcal{V}_{C,(L,T);\tau_N}}{1 - 2(f_\pi^2/m_\pi^2) \mathcal{V}_{C,(L,T);\tau_N} (Re\Pi_{nn}^0 + Re\Pi_{pp}^0 + iIm\Pi_{pp}^0)}.\end{aligned}\quad (4.26)$$

The next step is to study the configurations in the weak vertices. In this case, we should look at the particle-hole bubbles explicitly drawn in the *r.h.s* of Fig. 2 and 3. For $\Gamma_{n,n \rightarrow nn}$, these bubbles are replaced by Π_{nn}^0 . For $\Gamma_{p,p \rightarrow nn}$, the replacement is limited to $Re\Pi_{pp}^0$: as $j = nn$, all protons should be off the mass shell. Finally, for $\Gamma_{n,p \rightarrow nn}$ (or $\Gamma_{p,n \rightarrow nn}$), one bubble is replaced by Π_{nn}^0 and the other one by $Re\Pi_{pp}^0$. Using the same procedure for $j = np$, we have,

$$\begin{aligned}\tilde{\mathcal{U}}_{C,(L,T);\tau_N}^{nn \rightarrow nn,n}(q) &= (Re\{\Pi_{nn}^0\})^2 Im\{\tilde{\mathcal{V}}_{nn,C,(L,T);\tau_N}\} + \\ &\quad + 2 Re\{\Pi_{nn}^0\} Im\{\Pi_{nn}^0\} Re\{\tilde{\mathcal{V}}_{nn,C,(L,T);\tau_N}\} \\ \tilde{\mathcal{U}}_{C,(L,T);\tau_N}^{nn \rightarrow np,n}(q) &= (Re\{\Pi_{nn}^0\})^2 Im\{\tilde{\mathcal{V}}_{pp,C,(L,T);\tau_N}\}\end{aligned}$$

$$\begin{aligned}
\tilde{\mathcal{U}}_{C,(L,T);\tau_N}^{np \rightarrow nn,n}(q) &= Re\{\Pi_{pp}^0\} Im\{\tilde{\mathcal{V}}_{nn,C,(L,T);\tau_N} \Pi_{nn}^0\} \\
\tilde{\mathcal{U}}_{C,(L,T);\tau_N}^{np \rightarrow np,n}(q) &= Re\{\Pi_{nn}^0\} Im\{\tilde{\mathcal{V}}_{pp,C,(L,T);\tau_N} \Pi_{pp}^0\} \\
\tilde{\mathcal{U}}_{C,(L,T);\tau_N}^{pp \rightarrow nn,n}(q) &= (Re\{\Pi_{pp}^0\})^2 Im\{\tilde{\mathcal{V}}_{nn,C,(L,T);\tau_N}\} \\
\tilde{\mathcal{U}}_{C,(L,T);\tau_N}^{pp \rightarrow np,n}(q) &= (Re\{\Pi_{pp}^0\})^2 Im\{\tilde{\mathcal{V}}_{pp,C,(L,T);\tau_N}\} + \\
&\quad + 2 Re\{\Pi_{pp}^0\} Im\{\Pi_{pp}^0\} Re\{\tilde{\mathcal{V}}_{pp,C,(L,T);\tau_N}\} \\
\tilde{\mathcal{U}}_{C,(L,T);\tau_N}^{pp \rightarrow np,p}(q) &= (Re\{\Pi_{np}^0\})^2 Im\{\tilde{\mathcal{V}}_{np,C,(L,T);\tau_N}\} + \\
&\quad + 2 Re\{\Pi_{np}^0\} Im\{\Pi_{np}^0\} Re\{\tilde{\mathcal{V}}_{np,C,(L,T);\tau_N}\}
\end{aligned} \tag{4.27}$$

Finally, the summation over isospin leads to,

$$\begin{aligned}
\Gamma_{n,n \rightarrow nn} &= \tilde{\Gamma}_{111}^{n,n \rightarrow nn n} + \tilde{\Gamma}_{000}^{n,n \rightarrow nn n} + \tilde{\Gamma}_{110}^{n,n \rightarrow nn n} + \tilde{\Gamma}_{101}^{n,n \rightarrow nn n} + \tilde{\Gamma}_{011}^{n,n \rightarrow nn n} + \tilde{\Gamma}_{100}^{n,n \rightarrow nn n} + \\
&\quad + \tilde{\Gamma}_{010}^{n,n \rightarrow nn n} + \tilde{\Gamma}_{001}^{n,n \rightarrow nn n} \\
\Gamma_{n,p \rightarrow nn} &= \tilde{\Gamma}_{111}^{n,p \rightarrow nn n} + \tilde{\Gamma}_{000}^{n,p \rightarrow nn n} + \tilde{\Gamma}_{110}^{n,p \rightarrow nn n} - \tilde{\Gamma}_{101}^{n,p \rightarrow nn n} - \tilde{\Gamma}_{011}^{n,p \rightarrow nn n} - \tilde{\Gamma}_{100}^{n,p \rightarrow nn n} - \\
&\quad - \tilde{\Gamma}_{010}^{n,p \rightarrow nn n} + \tilde{\Gamma}_{001}^{n,p \rightarrow nn n} \\
\Gamma_{p,n \rightarrow nn} &= \tilde{\Gamma}_{111}^{p,n \rightarrow nn n} + \tilde{\Gamma}_{000}^{p,n \rightarrow nn n} - \tilde{\Gamma}_{110}^{p,n \rightarrow nn n} - \tilde{\Gamma}_{101}^{p,n \rightarrow nn n} + \tilde{\Gamma}_{011}^{p,n \rightarrow nn n} + \tilde{\Gamma}_{100}^{p,n \rightarrow nn n} - \\
&\quad - \tilde{\Gamma}_{010}^{p,n \rightarrow nn n} - \tilde{\Gamma}_{001}^{p,n \rightarrow nn n} \\
\Gamma_{p,p \rightarrow nn} &= \tilde{\Gamma}_{111}^{p,p \rightarrow nn n} + \tilde{\Gamma}_{000}^{p,p \rightarrow nn n} - \tilde{\Gamma}_{110}^{p,p \rightarrow nn n} + \tilde{\Gamma}_{101}^{p,p \rightarrow nn n} - \tilde{\Gamma}_{011}^{p,p \rightarrow nn n} - \tilde{\Gamma}_{100}^{p,p \rightarrow nn n} + \\
&\quad + \tilde{\Gamma}_{010}^{p,p \rightarrow nn n} - \tilde{\Gamma}_{001}^{p,p \rightarrow nn n} \\
\Gamma_{n,n \rightarrow np} &= \tilde{\Gamma}_{111}^{n,n \rightarrow np n} + \tilde{\Gamma}_{000}^{n,n \rightarrow np n} + \tilde{\Gamma}_{110}^{n,n \rightarrow np n} + \tilde{\Gamma}_{101}^{n,n \rightarrow np n} + \tilde{\Gamma}_{011}^{n,n \rightarrow np n} + \tilde{\Gamma}_{100}^{n,n \rightarrow np n} + \\
&\quad + \tilde{\Gamma}_{010}^{n,n \rightarrow np n} + \tilde{\Gamma}_{001}^{n,n \rightarrow np n} \\
\Gamma_{n,p \rightarrow np} &= \tilde{\Gamma}_{111}^{n,p \rightarrow np n} + \tilde{\Gamma}_{000}^{n,p \rightarrow np n} + \tilde{\Gamma}_{110}^{n,p \rightarrow np n} - \tilde{\Gamma}_{101}^{n,p \rightarrow np n} - \tilde{\Gamma}_{011}^{n,p \rightarrow np n} - \tilde{\Gamma}_{100}^{n,p \rightarrow np n} - \\
&\quad - \tilde{\Gamma}_{010}^{n,p \rightarrow np n} + \tilde{\Gamma}_{001}^{n,p \rightarrow np n} \\
\Gamma_{p,n \rightarrow np} &= \tilde{\Gamma}_{111}^{p,n \rightarrow np,n} + \tilde{\Gamma}_{000}^{p,n \rightarrow np,n} - \tilde{\Gamma}_{110}^{p,n \rightarrow np,n} - \tilde{\Gamma}_{101}^{p,n \rightarrow np,n} + \tilde{\Gamma}_{011}^{p,n \rightarrow np,n} + \tilde{\Gamma}_{100}^{p,n \rightarrow np,n} - \\
&\quad - \tilde{\Gamma}_{010}^{p,n \rightarrow np,n} - \tilde{\Gamma}_{001}^{p,n \rightarrow np,n} \\
\Gamma_{p,p \rightarrow np} &= 4 \tilde{\Gamma}_{111}^{p,p \rightarrow np,p} + \tilde{\Gamma}_{111}^{p,p \rightarrow np,n} + \tilde{\Gamma}_{000}^{p,p \rightarrow np,n} - \tilde{\Gamma}_{110}^{p,p \rightarrow np,n} + \tilde{\Gamma}_{101}^{p,p \rightarrow np,n} - \tilde{\Gamma}_{011}^{p,p \rightarrow np,n} - \\
&\quad - \tilde{\Gamma}_{100}^{p,p \rightarrow np,n} + \tilde{\Gamma}_{010}^{p,p \rightarrow np,n} - \tilde{\Gamma}_{001}^{p,p \rightarrow np,n}
\end{aligned} \tag{4.28}$$

The terms with 'mixed' isospin: we mean all terms but $\tilde{\Gamma}_{111}^{ii' \rightarrow j,n(p)}$ and $\tilde{\Gamma}_{000}^{ii' \rightarrow j,n(p)}$, are not null because of the summation over the isospin is truncated. If we sum up all terms with the same final state, these mixed terms cancel out.

C. Expressions for N_N and N_{NN}

From Eqs. (3.1-3.5), we finally have,

$$\begin{aligned}
N_n &= 2\bar{\Gamma}_n + \bar{\Gamma}_p + 2(\bar{\Gamma}_{n,n \rightarrow nn} + \bar{\Gamma}_{p,p \rightarrow nn} + \bar{\Gamma}_{n,p \rightarrow nn} + \bar{\Gamma}_{p,n \rightarrow nn}) + \\
&\quad + \bar{\Gamma}_{n,n \rightarrow np} + \bar{\Gamma}_{p,p \rightarrow np} + \bar{\Gamma}_{n,p \rightarrow np} + \bar{\Gamma}_{p,n \rightarrow np} \\
N_p &= \bar{\Gamma}_p + \bar{\Gamma}_{n,n \rightarrow np} + \bar{\Gamma}_{p,p \rightarrow np} + \bar{\Gamma}_{n,p \rightarrow np} + \bar{\Gamma}_{p,n \rightarrow np} \\
N_{nn} &= \bar{\Gamma}_n + \bar{\Gamma}_{n,n \rightarrow nn} + \bar{\Gamma}_{p,p \rightarrow nn} + \bar{\Gamma}_{n,p \rightarrow nn} + \bar{\Gamma}_{p,n \rightarrow nn} \\
N_{np} &= \bar{\Gamma}_p + \bar{\Gamma}_{n,n \rightarrow np} + \bar{\Gamma}_{p,p \rightarrow np} + \bar{\Gamma}_{n,p \rightarrow np} + \bar{\Gamma}_{p,n \rightarrow np}, \tag{4.29}
\end{aligned}$$

where we have employed again the normalization of Eq. (2.3). For completeness, from Eqs. (3.6-3.7),

$$\begin{aligned}
N_n^{1Bn} &= 2 + \frac{2\Gamma_{n,n \rightarrow nn} + \Gamma_{n,n \rightarrow np}}{\Gamma_n} \\
N_p^{1Bn} &= \frac{\Gamma_{n,n \rightarrow np}}{\Gamma_n} \\
N_n^{1Bp} &= 1 + \frac{2\Gamma_{p,p \rightarrow nn} + \Gamma_{p,p \rightarrow np}}{\Gamma_p} \\
N_p^{1Bp} &= 1 + \frac{\Gamma_{p,p \rightarrow np}}{\Gamma_p} \\
N_{nn}^{1Bn} &= 1 + \frac{\Gamma_{n,n \rightarrow nn}}{\Gamma_n} \\
N_{np}^{1Bn} &= \frac{\Gamma_{n,n \rightarrow np}}{\Gamma_n} \\
N_{nn}^{1Bp} &= \frac{\Gamma_{p,p \rightarrow nn}}{\Gamma_p} \\
N_{np}^{1Bp} &= 1 + \frac{\Gamma_{p,p \rightarrow np}}{\Gamma_p} \tag{4.30}
\end{aligned}$$

In the next section we give numerical results for these expressions.

V. RESULTS AND DISCUSSION

In this section we present the numerical results for the ratios N_n/N_p and N_{nn}/N_{np} , within the ring approximation. We use nuclear matter in addition to the LDA which allows us to discuss the ${}^{12}_\Lambda C$ hypernucleus. As already mentioned, the transition potential is represented by the exchanges of the π , η , K , ρ , ω and K^* -mesons. We have employed several nuclear residual interactions based on the OME. In particular, we have used the Bonn potential [36] in the framework of the parametrization presented in [37], which contains the exchange of π , ρ , σ and ω mesons, while the η and δ -mesons are neglected. In implementing the LDA, the hyperon is assumed to be in the $1s_{1/2}$ orbit of a harmonic oscillator well with frequency $\hbar\omega = 10.8$ MeV. As already stated, we have employed different values for the proton and neutron Fermi momenta, k_{F_n} and k_{F_p} , respectively.

Before we present our results, we summarize four models for the V^{NN} -strong potential:

- model 1: the Bonn potential [36] without SRC,
- model 2: the Bonn potential [36] with SRC,
- model 3: a $(\pi + \rho)$ -meson exchange potential with SRC.
- model 4: a $(\pi + \rho)$ -meson exchange potential without SRC, plus the g' -Landau-Migdal parameter. In particular, we have employed, $g' = 0.5$ (in pionic units).

In Table II we show values for N_n/N_p and N_{nn}/N_{np} . Our results underestimate the more recent data: $N_n/N_p = 2.00 \pm 0.09 \pm 0.14$ [8] and $N_{nn}/N_{np} = 0.53 \pm 0.13$ [11]. These experimental points have an energy threshold of $T_N^{th} = 60$ MeV and 30 MeV, respectively. However, a comparison with data is rather premature for reasons which are discussed soon. From this table, we notice that the inclusion of FSI improves the result. The SRC are important also for V^{NN} and as usually stated, this effect is well reproduced by the g' -Landau Migdal parameter. In this table, the results for Γ_n/Γ_p contain no Pauli-exchange terms, in order to be consistent with the ring approximation. The inclusion of exchange terms increases Γ_n/Γ_p from 0.274 to 0.285 [35].

In Table III we analyze the importance of the quantum-mechanical interference terms between the $\Lambda n \rightarrow nn$ and $\Lambda p \rightarrow np$ decay channels. The interference terms are more relevant for the *model* 1-interaction. The importance of the interference terms when SRC

TABLE II: Results for the ratios N_n/N_p and N_{nn}/N_{np} for ${}^{12}_\Lambda C$. In the first column we show the model for the nuclear interaction (see the text). In the second and third columns we quote the values for the Fermi momentum at $r = 0$ (in units of MeV/c) for neutrons and protons, respectively. In the columns $(N_n/N_p)^0$ and $(N_{nn}/N_{np})^0$ we show the results without FSI. We have also included the values for Γ_n/Γ_p .

| V^{NN} | $k_{F_n}(r = 0)$ | $k_{F_p}(r = 0)$ | Γ_n/Γ_p | $(N_n/N_p)^0$ | N_n/N_p | $(N_{nn}/N_{np})^0$ | N_{nn}/N_{np} |
|----------------|------------------|------------------|---------------------|---------------|-----------|---------------------|-----------------|
| <i>model 1</i> | 269.9 | 269.9 | 0.274 | 1.548 | 1.607 | 0.274 | 0.304 |
| <i>model 1</i> | 261.5 | 277.8 | 0.229 | 1.458 | 1.514 | 0.229 | 0.257 |
| <i>model 2</i> | <i>idem</i> | <i>idem</i> | <i>idem</i> | <i>idem</i> | 1.464 | <i>idem</i> | 0.232 |
| <i>model 3</i> | <i>idem</i> | <i>idem</i> | <i>idem</i> | <i>idem</i> | 1.462 | <i>idem</i> | 0.231 |
| <i>model 4</i> | <i>idem</i> | <i>idem</i> | <i>idem</i> | <i>idem</i> | 1.463 | <i>idem</i> | 0.231 |

are present, is reduced to approximately 1% for N_n/N_p and 2 – 3% for N_{nn}/N_{np} . When the SRC are eliminated, these percentages increase up to 4% and 12%, respectively. The SRC produce a quasi-cancellation of the interference terms. The trend, however, is that interference terms are more significant for N_{nn}/N_{np} .

TABLE III: Results for the ratios N_n/N_p and N_{nn}/N_{np} , with and without the interference terms between the $\Lambda n \rightarrow nn$ and $\Lambda p \rightarrow np$ amplitudes; where the last ones are denoted with the '*diag*' sub-index. The Fermi momenta at $r = 0$, are $k_{F_n} = 261.5$ and $k_{F_p} = 277.8$ MeV/c.

| V^{NN} | N_n/N_p | $(N_n/N_p)_{diag}$ | N_{nn}/N_{np} | $(N_{nn}/N_{np})_{diag}$ |
|----------------|-----------|--------------------|-----------------|--------------------------|
| <i>model 1</i> | 1.514 | 1.459 | 0.257 | 0.229 |
| <i>model 2</i> | 1.464 | 1.452 | 0.232 | 0.226 |
| <i>model 3</i> | 1.462 | 1.453 | 0.231 | 0.226 |

In Table IV, we report values for the $N_{N,(N_N)}^{1B_i}$ -factors from Eqs. (4.30). This is done

for two $V^{\Lambda N}$ -models: the one with only one pion exchange (OPE) and the complete OME. Through this table, we analyze the degree of dependence of these factors on the weak vertex. Before this analysis, we should note that the values for N_p^{1Bn} and N_p^{1Bp} are identical to those for N_{np}^{1Bn} and N_{np}^{1Bp} , respectively. This is a consequence and a limitation of the ring approximation, where the corresponding expressions are the same (see Eqs. (4.30)). The value for Γ_n/Γ_p changes from 0.167 (for OPE) to 0.229 (for OME), that is, a variation of 37%, while the same percentage is smaller for the more relevant $N_{N,(NN)}^{1Bi}$ -factors. However, it is clear that within our model, these factors depend on the weak vertex. To get a more clear understanding of the effect of this dependence, in Table V, we have employed the experimental values for N_n/N_p and N_{nn}/N_{np} together with the results in Table IV to get Γ_n/Γ_p from the Eqs.(2.12) and (2.13). We can see that the dependence on the weak vertex is negligible. In order to avoid confusion, let us summarize the main ideas. The INC calculation works in two sides: the theoretical one, in which the Γ_n/Γ_p -result depends on the weak vertex. And in second place, the search of a model independent value for Γ_n/Γ_p , which is called the experimental result for this ratio. This value is built up from the experimental value for N_n/N_p or N_{nn}/N_{np} and the results for the $N_{N,(NN)}^{1Bi}$ -factors, which should be as model independent as possible. Our analytical expressions for the $N_{N,(NN)}^{1Bi}$ -factors contradict the hypothesis of the independence of these factors on the weak vertex, but our numerical results confirm the possibility of a weak-vertex independent determination of the ratio Γ_n/Γ_p , in agreement with the INC calculation. Also from Table V, we can see that the values $(\Gamma_n/\Gamma_p)_{Eq. (2.12)}$ and $(\Gamma_n/\Gamma_p)_{Eq. (2.13)}$ are consistent within each other.

There are experimental information not only for the ratios N_n/N_p and N_{nn}/N_{np} but also for the N_n and N_p -spectra. In this contribution, we have preferred not to present results for the spectra yet. This is because, in developing a microscopic scheme to interpret the data, we have presented and discussed a formalism, where the numerical results are given within the ring approximation. This implementation should be seen as a first step towards more accurate results, which should care about:

- the inclusion of the Pauli-exchange terms,
- the addition of the two body-induced weak decays,
- the FSI, which should not be restricted to the ring approximation and

TABLE IV: Results of the $N_{N,(NN)}^{1Bi}$ -factors within the ring approximation. For the nuclear strong interaction we have taken the *model 1* one, where we have employed $k_{F_n} = 261.5$ and $k_{F_p} = 277.8$ MeV/c (at $r = 0$). In the line named as 'OPE' the $V^{\Lambda N}$ -transition potential is limited to a one pion-exchange. As already stated, the OME contains the complete pseudoscalar and vector meson octets ($\pi, \eta, K, \rho, \omega, K^*$).

| $V^{\Lambda N}$ | N_n^{1Bn} | N_p^{1Bn} | N_{nn}^{1Bn} | N_{np}^{1Bn} |
|---|-------------|-------------|----------------|----------------|
| OPE | 2.315 | 0.060 | 1.127 | 0.060 |
| OME | 2.299 | 0.055 | 1.122 | 0.055 |
| $(\Delta N_{N(N)}^{1Bi}/N_{N(N)}^{1Bi}) \times 100$ | 0.7 | 9.1 | 0.4 | 9.1 |
| $V^{\Lambda N}$ | N_n^{1Bp} | N_p^{1Bp} | N_{nn}^{1Bp} | N_{np}^{1Bp} |
| OPE | 1.201 | 1.174 | 0.013 | 1.174 |
| OME | 1.156 | 1.141 | 0.011 | 1.141 |
| $(\Delta N_{N(N)}^{1Bi}/N_{N(N)}^{1Bi}) \times 100$ | 3.9 | 2.9 | 18.2 | 2.9 |

TABLE V: The ratio Γ_n/Γ_p from Eqs. (2.12-2.13). The values for the $N_{N,(NN)}^{1Bi}$ -factors have been taken from Table IV and for N_n/N_p and N_{nn}/N_{np} , the data indicated in the text have been used.

| $V^{\Lambda N}$ | $(\Gamma_n/\Gamma_p)_{Eq. (2.12)}$ | $(\Gamma_n/\Gamma_p)_{Eq. (2.13)}$ |
|--|------------------------------------|------------------------------------|
| OPE | 0.52 ± 0.08 | 0.56 ± 0.14 |
| OME | 0.51 ± 0.07 | 0.54 ± 0.14 |
| $(\Delta(\Gamma_n/\Gamma_p)/(\Gamma_n/\Gamma_p)) \times 100$ | ~ 2 | ~ 3 |

- the energy threshold used to obtain the data.

The Pauli-exchange terms. In [35], we have shown that Pauli exchange terms are important. In that work, a full antisymmetric calculation for the evaluation of Γ_n and Γ_p has been done.

As it is well known, the ring approximation is the direct part of the RPA. In [38], it has been established that the RPA-exchange terms are also important. Even though the physical process studied in that work is different, the kinematical conditions are similar: in both cases the momentum carried by the nuclear interaction is of the order of 400 MeV/c. From this fact, we can conclude that there is a priori no reason to neglect the RPA-exchange terms. Nevertheless, the implementation of the RPA in the present problem is quite an involved task. The advantage of the ring series is that it can be summed up to infinite order. Once exchange terms are incorporated, the RPA-series can not be summed for a general finite range nuclear interaction and each term should be computed individually. Even for the lowest order RPA-contribution, there are three two-body operators: the nuclear strong interaction V^{NN} , and the transition potential $V^{\Lambda N}$ (which appears twice). As for each operator there is a direct and an exchange matrix element, one has to evaluate eight terms. The RPA (or the lowest order contribution to it), is beyond the scope of the present work, though a fair comparison with data should certainly contain antisymmetrization.

Two body-induced decays. The non-mesonic weak decay of the Λ is not only induced by the process $\Lambda N \rightarrow NN$ but also by the two-nucleon induced decay, $\Lambda NN \rightarrow NNN$. If we call Γ_2 this decay width, then the total non-mesonic decay width should be corrected as, $\Gamma_{NM} = \Gamma_n + \Gamma_p + \Gamma_2$. This last mechanism is originated from ground state correlations and in [30], we have shown that this decay is $\sim 24\%$ of the total non-mesonic decay width. From these simple considerations it is clear that the two body-induced decay plays a relevant role in the evaluation of N_N and N_{NN} , a point which has been already discussed in [33]. The modifications in our expressions to include this decay channel are simple. However, the problem here is the huge number of possible diagrams which should be considered.

The model for the FSI. The FSI admits two different approaches: one is the semi-phenomenological INC calculation and the other one is a microscopic treatment like ours. It is not possible to establish a biunique relation between the processes in both models. We focus on the microscopic point of view, and within this approach the ring approximation constitutes a very particular set of diagrams which contributes to the FSI. There are also FSI beyond the ring approximation which are important. For instance, this issue is addressed in [29], where the bosonic loop expansion formalism is employed. However, and as it is mentioned in that very same work, within this scheme it is difficult to disentangle two-nucleon from three-nucleon final states. Obviously, the same consideration stated at the

end of the last paragraph, with respect to the number of possible diagrams, is held here. In spite of these difficulties, we want to stress that the final goal of our formalism (given by Eqs. (3.1)-(3.5)), is the evaluation of FSI more complex than the ring approximation or the RPA.

The energy threshold. The Λ within the hypernucleus can decay either through the mesonic or through the non-mesonic decay. In both cases, at least one nucleon is produced. Obviously, the detectors can not distinguish between nucleons coming from the mesonic and the non-mesonic decay. Fortunately, the value for the energy of the nucleons from the mesonic decay is small. Due to experimental conditions, up to now particles with energy smaller than 30 MeV, can not be detected. This energy threshold is big enough to eliminate all particles coming from the mesonic decay. The numerical implementation of this threshold is not difficult: in the expressions for the decay widths, two step functions should be added to guarantee that the energy of the emitted particles is greater than the threshold. In any case, this threshold affects the neutron- and proton-spectra, more than the ratios N_n/N_p and N_{nn}/N_{np} . For this reason, together with the will of making our presentation less complex, we have omitted its inclusion.

From all these points, we wanted to emphasize that there are several topics to overcome before we attempt a more realistic comparison with data. The same consideration holds if we compare our results with the ones from the INC calculation. Throughout the present contribution, the INC calculation has been taken as a reference guide. In spite of this, the INC calculation is essentially different from our approach: in the INC calculation once the Λ -decays, the trajectory of the emitted nucleons are followed in their way out of the nucleus. The free paths of these nucleons and their collisions cross sections, are considered. From the four points mentioned above, the effect of the second, third and fourth points are incorporated within the INC calculation. Due to its semi-classical character, the first point together with some interference terms can not be taken into account. At variance, because of the quantum-mechanical character of our scheme, the concept of trajectory is not applicable for us. In our case, by means of the LDA, we allow the decay to take place in any point of the hypernucleus. After the weak decay occurs, it follows the usual many-body problem; which requires the election of certain sets of diagrams together with the election of a nuclear residual interaction. Here and as a first step, we have implemented the ring approximation.

VI. CONCLUSIONS

In this work we have addressed the problem of the non-mesonic weak decay of Λ -hyper-nuclei. As a result of the Λ -decay, nucleons are emitted from the nucleus and these nucleons can be measured. Moreover, nucleons from the non-mesonic weak decay can be disentangled from those originated in the mesonic decay. We represent with N_N and N_{NN} the number of nucleons of kind N and the number of pairs of nucleons of kind NN , respectively. We have developed for the first time a microscopic model for N_N and N_{NN} , using non-relativistic nuclear matter. The interference terms between the n - and p -induced weak decay widths are automatically taken into account in our scheme. Explicit expressions and numerical results are given within the ring approximation together with the LDA. Due to the limitations inherent to the ring approximation, our numerical results should be seen as preliminary. Our values for the ratios N_n/N_p and N_{nn}/N_{np} underestimate the data. Our results do not contain an energy threshold, but a threshold should affect the N_n and N_p -spectrum, more than the mentioned ratios. Within the same model, our value for Γ_n/Γ_p is in the range $0.2 - 0.3$.

It is our opinion that the so-called Γ_n/Γ_p -puzzle has been misinterpreted. In the literature, the theoretical predictions for Γ_n/Γ_p are smaller than 0.5. Old reported data for this ratio are closer to one. More experiments have been done and much theoretical effort has been employed in the hope that the experiments produce smaller values and/or theory predicts bigger ones. The missing piece of this puzzle is the link between theory and experiment. The INC calculation address this point, but it gives a different treatment to the weak decay and to the subsequent nuclear many-body problem. The INC calculation is not able to evaluate the interference terms between the n - and p -induced weak decay widths. In fact, these terms have never been evaluated before. Our results show that these terms can be neglected when SRC are present and within the ring approximation.

Besides these considerations, one question remains. And it is if Γ_n/Γ_p is an observable or not. Certainly, it is not possible to perform a direct measurement of the number of particles emitted in the weak decay vertex: Γ_n/Γ_p is obtained indirectly. Now, if several models produce the same Γ_n/Γ_p -result using the same experimental information, then it would be fair to call this number, the experimental result for Γ_n/Γ_p . In the INC calculation, for instance, the first step is the theoretical evaluation of the $N_{n(p)}^{1\text{Bn}(p)}$ -factors. Then, they

are used together with the data for N_n/N_p (or N_{nn}/N_{np}), in Eq. (2.12) (or (2.13)) to obtain the so-called experimental result for the ratio Γ_n/Γ_p (which is compared with the theoretical determinations of it). Anyway, in the present contribution we have tried to present an alternative point of view on this subject. We calculate N_n/N_p and N_{nn}/N_{np} which are straightaway compared with data. Therefore, Γ_n and Γ_p are ingredients within our model. Regarding the question about whether or not Γ_n/Γ_p is observable, is of secondary importance: once the data for N_n/N_p and N_{nn}/N_{np} , together with the corresponding spectra, are well understood, the disagreement between the theoretical and the so-called experimental value for Γ_n/Γ_p would disappear automatically.

Then, as mentioned, we have presented a unified model which evaluates Γ_n/Γ_p , N_n/N_p and N_{nn}/N_{np} . This model is summarized in Eqs. (3.1)-(3.5). We have called attention on the fact that several improvements over the ring approximation should be implemented before we attempt a more realistic comparison with data. From these points, the inclusion of the Pauli exclusion principle should be the first step. We believe that, in spite of the difficulties inherent to the nuclear many-body problem, we have shown that our proposal is feasible. We also believe that the nuclear many-body problem after the weak decay take place, is as important as the weak decay itself.

Acknowledgments

I would like to thank F. Krmpotić for fruitful discussions and for the critical reading of the manuscript. This work has been partially supported by the CONICET, under contract PIP 6159.

APPENDIX

In this Appendix we show some details about the derivation of the $\tilde{\mathcal{S}}_{\tau\tau_N\tau'}^{i,i'\rightarrow j,(n,p)}(q)$ -functions (Eqs. (4.24)-(4.25)). The starting point is Eq. (4.17). By performing the energy integration, using the factorization (4.20) (which separates the isospin matrix elements), the expressions for the transition potential and the nuclear interaction given by Eqs. (4.3) and (4.16), respectively and after some algebra, we have,

$$\begin{aligned} \tilde{\Gamma}_{\tau\tau_N\tau'}^{i,i'\rightarrow j,n}(k, k_{F_n}, k_{F_p}) &= \frac{-2}{(2\pi)^9} \frac{1}{4} \sum_{all\ spin} Im \int d\mathbf{p}_1 \int d\mathbf{h}_i \int d\mathbf{h}_{i'} \theta(q_0) \theta(|\mathbf{p}_1| - k_{F_n}) \\ &\times \frac{\theta(|\mathbf{h}_i + \mathbf{q}| - k_{F_{t_{p_1}}}) \theta(k_{F_{t_{h_i}}} - |\mathbf{h}_i|)}{q_0 - (E_N(\mathbf{h}_i + \mathbf{q}) - E_N(\mathbf{h}_i)) + i\eta} \\ &\times \frac{\theta(|\mathbf{h}_{i'} + \mathbf{q}| - k_{F_{t_{p_{i'}}}}) \theta(k_{F_{t_{h_{i'}}}} - |\mathbf{h}_{i'}|)}{q_0 - (E_N(\mathbf{h}_{i'} + \mathbf{q}) - E_N(\mathbf{h}_{i'})) + i\eta} \\ &\times \langle s_\Lambda | (\mathcal{V}_\tau^{\Lambda N}(q))^\dagger | s_{p_1} s_{p_{i'}} s_{h_{i'}} \rangle \langle s_{p_1} s_{p_{i'}} s_{h_{i'}} | \tilde{\mathcal{V}}_{\tau_N}^{NN}(q) | s_{p_1} s_{p_i} s_{h_i} \rangle \\ &\times \langle s_{p_1} s_{p_i} s_{h_i} | \mathcal{V}_{\tau'}^{\Lambda N}(q) | s_\Lambda \rangle. \end{aligned} \quad (6.1)$$

and

$$\begin{aligned} \tilde{\Gamma}_{\tau\tau_N\tau'}^{i,i'\rightarrow j,p}(k, k_{F_n}, k_{F_p}) &= \frac{-2}{(2\pi)^9} \frac{1}{4} \sum_{all\ spin} Im \int d\mathbf{p}_1 \int d\mathbf{h}_i \int d\mathbf{h}_{i'} \theta(q_0) \theta(|\mathbf{p}_1| - k_{F_p}) \\ &\times \frac{\theta(|\mathbf{h}_i + \mathbf{q}| - k_{F_n}) \theta(k_{F_p} - |\mathbf{h}_i|)}{q_0 - (E_N(\mathbf{h}_i + \mathbf{q}) - E_N(\mathbf{h}_i)) + i\eta} \\ &\times \frac{\theta(|\mathbf{h}_{i'} + \mathbf{q}| - k_{F_n}) \theta(k_{F_p} - |\mathbf{h}_{i'}|)}{q_0 - (E_N(\mathbf{h}_{i'} + \mathbf{q}) - E_N(\mathbf{h}_{i'})) + i\eta} \\ &\times \langle s_\Lambda | (\mathcal{V}_\tau^{\Lambda N}(q))^\dagger | s_{p_1} s_{p_{i'}} s_{h_{i'}} \rangle \langle s_{p_1} s_{p_{i'}} s_{h_{i'}} | \tilde{\mathcal{V}}_{\tau_N}^{NN}(q) | s_{p_1} s_{p_i} s_{h_i} \rangle \\ &\times \langle s_{p_1} s_{p_i} s_{h_i} | \mathcal{V}_{\tau'}^{\Lambda N}(q) | s_\Lambda \rangle. \end{aligned} \quad (6.2)$$

where $k_0 = E_\Lambda(\mathbf{k}) + V_\Lambda$ and $\mathbf{q} = \mathbf{p}_1 - \mathbf{k}$. Now, the integrations over \mathbf{h}_i and $\mathbf{h}_{i'}$ are replaced by the function $\Pi^0 t_{p_i(i')} t_{h_i(i')}(q)$ (Eq. (4.11)). Summing up in spin, we have,

$$\begin{aligned} \tilde{\Gamma}_{\tau\tau_N\tau'}^{i,i'\rightarrow j,n}(k, k_{F_n}, k_{F_p}) &= (G_F m_\pi^2)^2 \left(\frac{f_\pi^2}{m_\pi^2}\right) \frac{-1}{(2\pi)^2} Im \int d\mathbf{p}_1 \theta(q_0) \theta(|\mathbf{p}_1| - k_{F_n}) \Pi^0 t_{p_i} t_{h_i}(q) \\ &\times \Pi^0 t_{p_{i'}} t_{h_{i'}}(q) \{ (S'_\tau S'_{\tau'} + P_{C,\tau} P_{C,\tau'}) \tilde{\mathcal{V}}_{t_p t_h, C; \tau_N} + (S_\tau S_{\tau'} + P_{L,\tau} P_{L,\tau'}) \\ &\times \tilde{\mathcal{V}}_{t_p t_h, L; \tau_N} + 2 (S_{V,\tau} S_{V,\tau'} + P_{T,\tau} P_{T,\tau'}) \tilde{\mathcal{V}}_{t_p t_h, T; \tau_N} \} \end{aligned} \quad (6.3)$$

and

$$\tilde{\Gamma}_{\tau\tau_N\tau'}^{i,i'\rightarrow j,p}(k, k_{F_n}, k_{F_p}) = (G_F m_\pi^2)^2 \left(\frac{f_\pi^2}{m_\pi^2}\right) \frac{-1}{(2\pi)^2} Im \int d\mathbf{p}_1 \theta(q_0) \theta(|\mathbf{p}_1| - k_{F_p}) \Pi_{np}^0(q) \Pi_{np}^0(q)$$

$$\begin{aligned}
& \times \{ (S'_\tau S'_{\tau'} + P_{C,\tau} P_{C,\tau'}) \tilde{\mathcal{V}}_{np,C;\tau_N} + (S_\tau S_{\tau'} + P_{L,\tau} P_{L,\tau'}) \tilde{\mathcal{V}}_{np,L;\tau_N} + \\
& + 2 (S_{V,\tau} S_{V,\tau'} + P_{T,\tau} P_{T,\tau'}) \tilde{\mathcal{V}}_{np,T;\tau_N} \} \tag{6.4}
\end{aligned}$$

where the functions $\tilde{\mathcal{V}}_{t_p t_h, C(L,T);\tau_N}(q)$ are defined in Eq. (4.26). The isospin is analyzed in detail in Section IV B.

By comparison of Eqs. (6.3) and (6.4) with Eqs. (4.22) and (4.23), respectively, it is straightforward to obtain the expressions for $\tilde{\mathcal{S}}_{\tau\tau_N\tau'}^{i,i'\rightarrow j,n(p)}(q)$ and $\tilde{\mathcal{U}}_{C(L,T);\tau_N}^{i,i'\rightarrow j,n(p)}(q)$.

-
- [1] M. Danysz and J. Pniewski, *Philos. Mag.*, **44**, 348 (1953).
- [2] E. Oset and A. Ramos, *Prog. Part. Nucl. Phys.* **41**, 191 (1998).
- [3] W. M. Alberico and G. Garbarino, *Phys. Rep.* **369**, 1 (2002); in *Hadron Physics*, IOS Press, Amsterdam, 125 (2005). Edited by T. Bressani, A. Filippi and U. Wiedner. Proceedings of the International School of Physics “Enrico Fermi”, Course CLVIII, Varenna (Italy), June 22 – July 2, 2004.
- [4] A. Montwill et al., *Nucl. Phys. A* **234**, 413 (1974).
- [5] O. Hashimoto et al., *Phys. Rev. Lett.* **88**, 042503 (2002).
- [6] Y. Sato et al., *Phys. Rev. C* **71**, 025203 (2005).
- [7] J. H. Kim et al., *Phys. Rev. C* **68**, 065201 (2003).
- [8] S. Okada et al., *Phys. Lett. B* **597**, 249 (2004).
- [9] H. Bhang, in *DAPHNE 2004: Physics at meson factories*, Frascati Phys. Ser. **36**, 243 (2005). Edited by F. Anulli, M. Bertani, G. Capon, C. Curceanu–Petrascu, F. L. Fabbri and S. Miscetti.
- [10] H. Ota, in *Hadron Physics* p. 219; H. Ota et al., *Nucl. Phys. A* **754**, 157c (2005).
- [11] B. H. Kang et al., *Phys. Rev. Lett.* **96**, 062301 (2006).
- [12] M. J. Kim et al., nucl-ex/0601029.
- [13] J. B. Adams, *Phys. Rev.* **156**, 1611 (1967).
- [14] B. H. J. McKellar and B. F. Gibson, *Phys. Rev. C* **30**, 322 (1984).
- [15] J. F. Dubach, G. B. Feldman, B. R. Holstein and L. de la Torre, *Ann. Phys.* **249**, 146 (1996).
- [16] A. Parreño, A. Ramos and C. Bennhold, *Phys. Rev. C* **56**, 339 (1997).
- [17] D. Jido, E. Oset and J. E. Palomar, *Nucl. Phys. A* **694**, 525 (2001).
- [18] A. Parreño and A. Ramos, *Phys. Rev. C* **65**, 015204 (2002).
- [19] K. Itonaga, T. Ueda, and T. Motoba, *Phys. Rev. C* **65**, 034617 (2002).
- [20] K. Maltman and M. Shmatikov, *Phys. Lett. B* **331**, 1 (1994).
- [21] T. Inoue, S. Takeuchi and M. Oka, *Nucl. Phys. A* **577**, 281c (1994); *ibid.* **A 597**, 563 (1996).
T. Inoue, M. Oka, T. Motoba and K. Itonaga, *Nucl. Phys. A* **633**, 312 (1998). T. Inoue, M. Oka, T. Motoba and K. Itonaga, *Nucl. Phys. A* **633**, 312 (1998).
- [22] J. Golak, K. Miyagawa, H. Kamada, H. Witala, W. Glöckle, A. Parreño, A. Ramos and C.

- Bennhold, Phys. Rev. **C 55**, 2196 (1997).
- [23] A. Parreño, A. Ramos, C. Bennhold and Maltman, Phys. Lett. **B 435**, 1 (1998).
- [24] K. Sasaki, T. Inoue and M. Oka, Nucl. Phys. **A 669**, 331 (2000); **678**, 455(E) (2000); Nucl. Phys. **A 707**, 477 (2002).
- [25] W. M. Alberico, A. De Pace, M. Ericson and A. Molinari, Phys. Lett. **B 256**, 134 (1991).
- [26] A. Ramos, E. Oset and L. L. Salcedo, Phys. Rev. **C 50**, 2314 (1994).
- [27] A. Ramos, M. J. Vicente-Vacas and E. Oset, Phys. Rev. **C 55**, 735 (1997); **66**, 039903(E) (2002).
- [28] W. M. Alberico, A. De Pace, G. Garbarino and A. Ramos, Phys. Rev. **C 61**, 044314 (2000).
- [29] W. M. Alberico, A. De Pace, G. Garbarino and R. Cenni, Nucl. Phys. **A 668**, 113 (2000).
- [30] E. Bauer and F. Krmpotić, Nucl. Phys. **A 739**, 109 (2004).
- [31] G. Garbarino, A. Parreño and A. Ramos, Phys. Rev. Lett. **91**, 112501 (2003).
- [32] G. Garbarino, A. Parreño and A. Ramos, Phys. Rev. **C 69**, 054603 (2004).
- [33] E. Bauer, G. Garbarino, A. Parreño and A. Ramos, nucl-th/0602066.
- [34] E. Oset and L. L. Salcedo, Nucl. Phys. **A 443**, 704 (1985).
- [35] E. Bauer and F. Krmpotić, Nucl. Phys. **A 717**, 217 (2003).
- [36] R. Machleidt, K. Holinde and Ch. Elster; Phys. Rep. **149**, 1 (1987).
- [37] M. B. Barbaro, A. De Pace, T. W. Donnelly and A. Molinari, Nucl. Phys. **A 596**, 553 (1996).
- [38] E. Bauer, A. Ramos and A. Polls, Phys. Rev. **C 54**, 2959 (1996).